# Journal Pre-proof


Design, synthesis and evaluation of phenylthiazole and phenylthiophene pyrimidindiamine derivatives targeting the bacterial membrane

Tingting Fan, Weikai Guo, Ting Shao, Wenbo Zhou, Pan Hu, Mingyao Liu, Yihua Chen, Zhengfang Yi

PII: S0223-5234(20)30108-2

DOI: https://doi.org/10.1016/j.ejmech.2020.112141

Reference: EJMECH 112141

To appear in: *European Journal of Medicinal Chemistry*

Received Date: 31 December 2019

Revised Date: 10 February 2020

Accepted Date: 10 February 2020

Please cite this article as: T. Fan, W. Guo, T. Shao, W. Zhou, P. Hu, M. Liu, Y. Chen, Z. Yi, Design, synthesis and evaluation of phenylthiazole and phenylthiophene pyrimidindiamine derivatives targeting the bacterial membrane, *European Journal of Medicinal Chemistry* (2020), doi: https://doi.org/10.1016/j.ejmech.2020.112141.

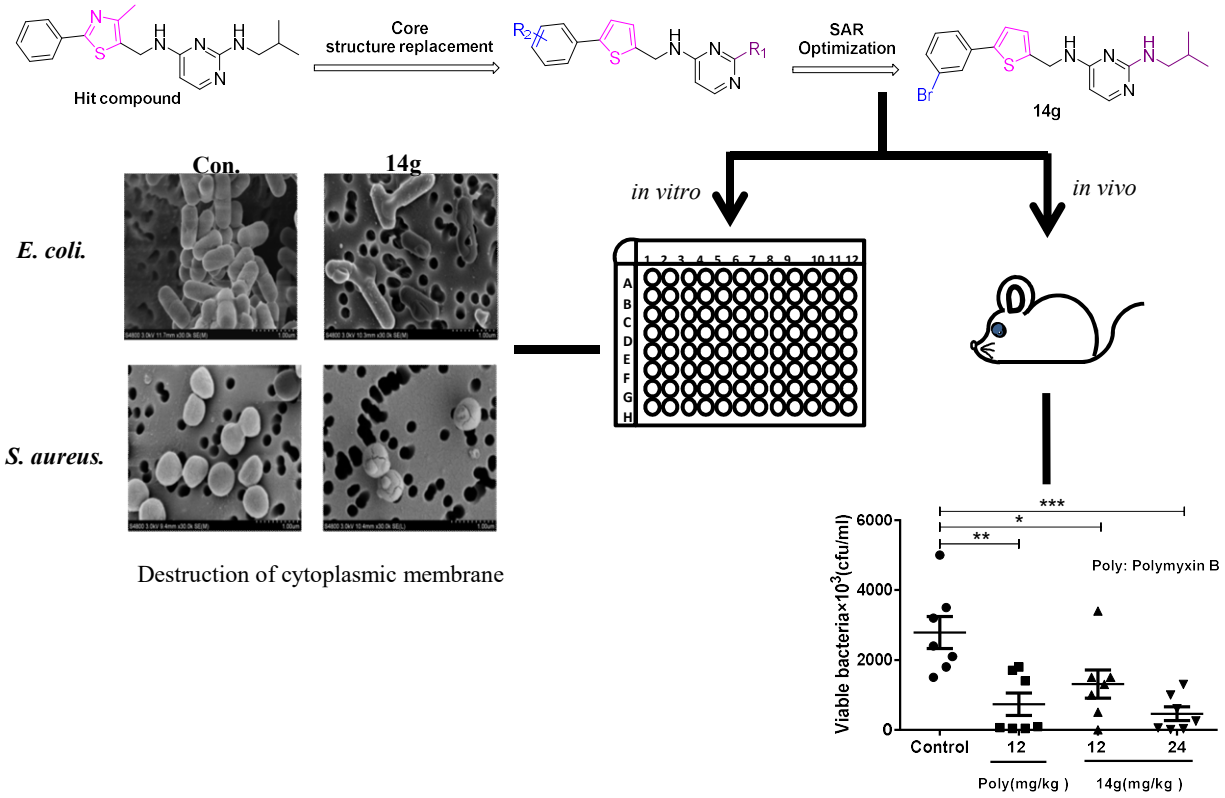
Hit compound
Core
structure replacement
SAR
Optimization
14g
Con.
14g
E. coli.
S. aureus.
in vitro
in vivo
Destruction of cytoplasmic membrane
Viable bacteria×10³(cfu/ml)
6000
4000
2000
0
***
*
**
Poly: Polymyxin B
Control
12
12
24
Poly(mg/kg )
14g(mg/kg )
Elimination of viable pathogens

# Design, synthesis and evaluation of phenylthiazole and phenylthiophene pyrimidindiamine derivatives targeting the bacterial membrane

Tingting Fan[a,b,1], Weikai Guo[a,1], Ting Shao[a], Wenbo Zhou[a], Pan Hu[a], Mingyao Liu[a], Yihua Chen[a]* and Zhengfang Yi[a]*

[a]*East China Normal University and Shanghai Fengxian District Central Hospital Joint Center for Translational Medicine, Shanghai Key Laboratory of Regulatory Biology, Institute of Biomedical Sciences and School of Life Sciences, East China Normal University, 200241 Shanghai, China*

[b]*Changzhi Medical College, Changzhi 046000, Shanxi, China*

*Corresponding authors.

*Z.Y.: Phone: +86-21-54345016. Fax: +86-21-54344922. E-mail: zfyi@bio.ecnu.edu.cn

*Y.C.: Phone: +86-21-24206647. Fax: +86-21-54344922. E-mail: yhchen@bio.ecnu.edu.cn

[1]These authors contributed equally to this work.

***Keywords*:** Antibacterial activity, Thiazole, Thiophene, Membrane damage

**ABSTRACT**

As the continuous rise in the incidence of antibiotic resistance, it is urgent to develop novel chemical scaffolds with antibacterial activities to control the spread of resistance to conventional antibiotics. In this study, a series of phenylthiazole and phenylthiophene pyrimidindiamine derivatives were designed and synthesized by modifying the hit compound ($N^2$-isobutyl-$N^4$-((4-methyl-2-phenylthiazol-5-yl)methyl) pyrimidine-2,4-diamine) and their antibacterial activities were evaluated both *in vitro* and *in vivo*. Among the tested compounds, compound **14g** ($N^4$-((5-(3-bromophenyl)thiophen-2-yl)methyl)-$N^2$-isobutylpyrimidine-2,4-diamine) displayed the best antibacterial activities, which was not only capable of inhibiting *E. coli* and *S. aureus* growth at concentrations as low as 2 and 3 μg/mL *in vitro*, but also efficacious in a mice model of bacteremia *in vivo*. Unlike conventional antibiotics, compound **14g** was elucidated to mainly destroy the bacterial cell membrane, with the dissipation of membrane potential and leakage of contents, ultimately leading to cell death. The destruction of cell structure is challenging to induce bacterial resistance, which suggested that compound **14g** may be a kind of promising alternatives to antibiotics against bacteria.

## 1. Introduction

Antibiotics have been essential life-saving drugs to revolutionize medicine radically [1]. Indeed, since the discovery of penicillin in 1928, several highly effective antibiotics have been developed for clinical treatments of bacterial infections [2]. It is estimated that the widespread use of antibiotics has extended human life expectancy

by about 30 years in the developed countries [3]. However, the extensive availability of antibiotics has also caused many uncontrollable adverse effects [4], the most serious of which is the induction of bacterial resistance [5, 6]. The efficacies of drugs will be severely reduced or even invalidated once bacterial resistance occurs [7]. Numerous researches pointed out that bacterial resistance to antibiotics has reached alarming levels worldwide [8-12]. It was suggested that the number of deaths due to bacterial resistance might increase from the current estimated 700,000 to 10,000,000 annually by 2050 [13]. There is little way to stop bacteria from developing adaptation to the environment and antibiotics [14, 15]. The continuous development of new drugs to keep pace with, or even exceed the evolution and spread of bacterial resistance is widely recognized as one of the effective strategies to prevent the dawn of the post-antibiotic era. However, there are few new drugs currently in the discovery and clinical pipeline, as natural antibiotics are difficult and expensive to synthesize or isolate [16]. What's worse, most of the current drug developments are based on the modification of existing antibiotic structures, which are easy to induce resistance again with a high probability of cross-resistance [7]. Therefore, designing and discovering more novel antibacterial agents with different scaffolds are urgent to alleviate this situation.

In this study, to discover novel antibacterial candidates with different skeletons from traditional antibiotics, an in-house library of more than 200 newly synthesized compounds was screened based on their antibacterial effects at lower dilutions. As a result, the hit compound $N^2$-isobutyl-$N^4$-((4-methyl-2-phenylthiazol-5-yl)methyl)

pyrimidine-2,4-diamine displayed mild antibacterial activities against *Escherichia coli* (*E. coli*) and *Staphylococcus aureus* (*S. aureus*) with minimum inhibitory concentration (MIC) of 16 μg/mL (Fig. 1). As been known, the 2,4-pyrimidindiamine scaffold has existed in several antibacterials, such as trimethoprim **a** (**TMP**) [17], Mycobacterial dihydrofolate reductase inhibitor **b** (**SRI-20094**) [18], and Bacillus anthracis dihydrofolate reductase inhibitors **c** [19] and **d** [20] (Fig. 1). Besides, a series of hybrid of tetrahydrocarbazole with 2,4-diaminopyrimidine scaffold has also shown antibacterial activities in our previous studies [21]. To further optimize the antibacterial activities and explore the structure-activity relationship, a series of phenylthiazole and phenylthiophene pyrimidindiamine derivatives were designed and synthesized based on the hit compound. Firstly, it was investigated for the positions of the diaminopyrimidinyl group linking to the thiazole ring as well as their antibacterial activities. Secondly, we replaced the thiazole ring with the thiophene ring and modified the substitutions in pyrimidine ring at 2-position and that in phenyl ring at the left part. Among them, compound **14g** showed the most antibacterial effects with MIC value of 2 and 3 μg/mL for *E. coli* and *S. aureus*, respectively.

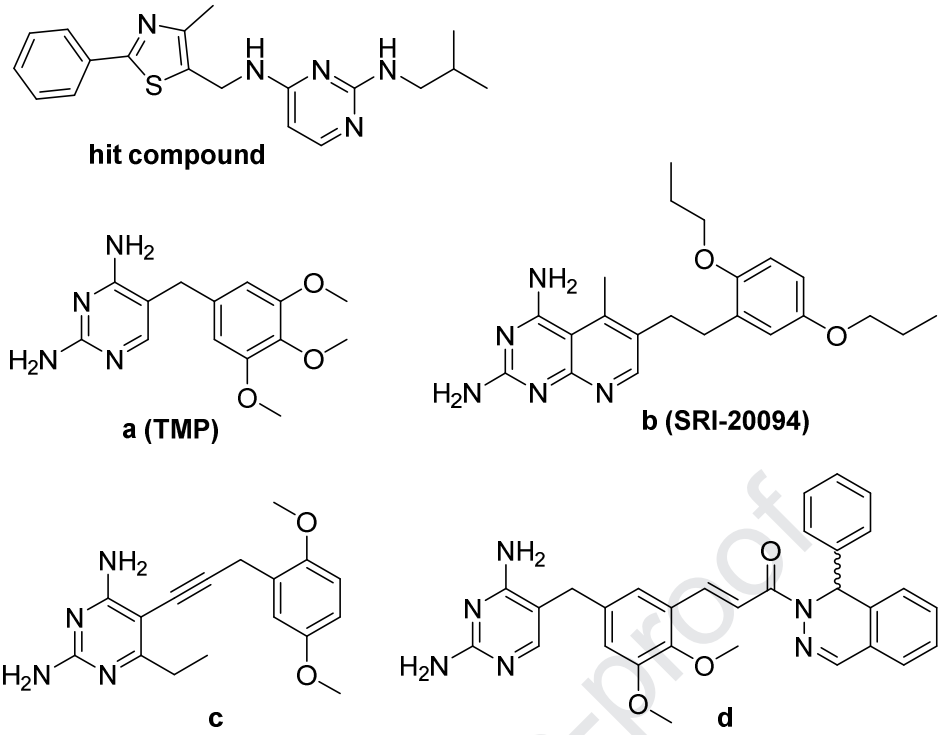


**Fig 1.** The structure of the hit compound as well as several known antimicrobial agents with diaminopyrimidine skeleton.

The conventional antibiotics primarily exert antibacterial effect by entering cells and interfering with the physiological activities in the cells, such as inhibiting cell wall synthesis, DNA replication and protein synthesis, thus giving bacteria chance to get tolerance by changing drug targets, preventing drugs from entering, and degrading drugs [22]. In contrast, compound **14g** was found to achieve antibacterial effects mainly by destroying the bacterial cell membrane structure. The cell membranes are essential material guarantees for intracellular physiological activities, increasing studies have focused on the development of membrane-active compounds with a broad-spectrum activity [23, 24]. The normal physiological function of incomplete membranes will be interrupted because there are many important proteins distributed on the cell membrane and the increased membrane permeability will promote the

entry of other drugs to produce a synergistic effect [25]. These may contribute to the antibacterial efficacy of compound **14g**. Furthermore, the membrane-active compounds can overcome non-inherited antibiotic resistance since both actively dividing cells and non-dividing cells need intact membranes to remain viable [26], and there is little chance for inactive bacterial cells to develop resistance [24, 27, 28]. Hence, compound **14g** with a novel structure and acting by destroying the cell membrane can minimize the emergence of resistance. This study is meaningful for the development of new antibacterial drugs in the future.

## 2. Chemistry

The synthetic route of compounds **6** and **7** was shown in Scheme 1. Thiobenzamide **1** was condensed with ethyl bromopyruvate to give the critical intermediate ethyl 2-phenylthiazole-4-carboxylate **2**. Compound **3** was obtained by reducing **2** with $LiAlH_4$, and then it was brominated with phosphorus tribromide to afford **4**, which was subsequently converted to the relevant amine **5** via Gabriel reaction. Compound **5** was coupled with 2,4-dichloropyrimidine to yield target compound **6**, which was underwent a nucleophilic substitution reaction with isobutylamine to produce **7**.

Synthesis of the compounds **13a-k** and **14a-h** followed the general procedures illustrated in Scheme 2. Different boronic acids were undergone Suzuki coupling reactions with bromothiophene derivatives to afford compound **9**. Subsequently, the treatment of compound **9** with hydroxylamine hydrochloride generated compound **10**, which was further reduced to obtain compound **11**. Compound **12** was prepared

through coupling **11** with 2,4-dichloropyrimidine, which was underwent similar nucleophilic substitution reactions with different amines to produce compounds **13a-k** and **14a-h**.

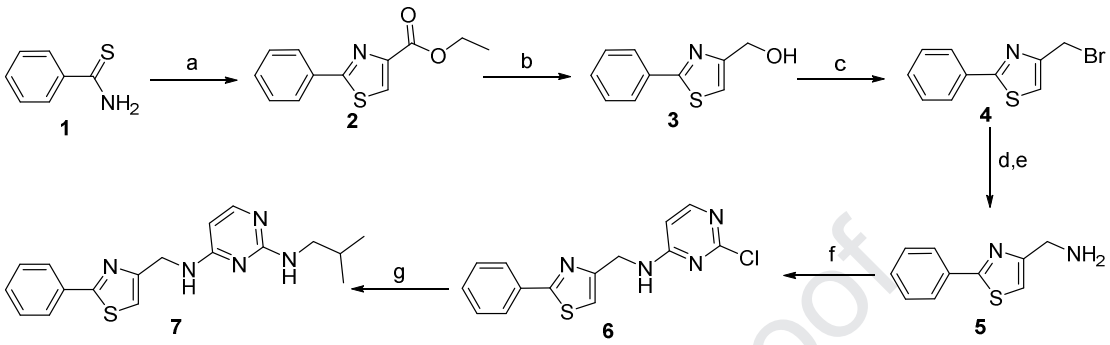


**Scheme 1**. Synthesis of compounds **6** and **7**. Reagents and conditions: (a) ethyl bromopyruvate, EtOH, reflux; (b) $LiAlH_4$, $Et_2O$, 0 °C then to r.t; (c) $PBr_3$, DCM, r.t; (d) potassium phthalimide, DMF, 60 °C; (e) $NH_2NH_2{\cdot}H_2O$, reflux; (f) 2,4-dichloropyrimidine, DIEA, EtOH, 40 °C; (g) isobutylamine, DIEA, n-BuOH, reflux.

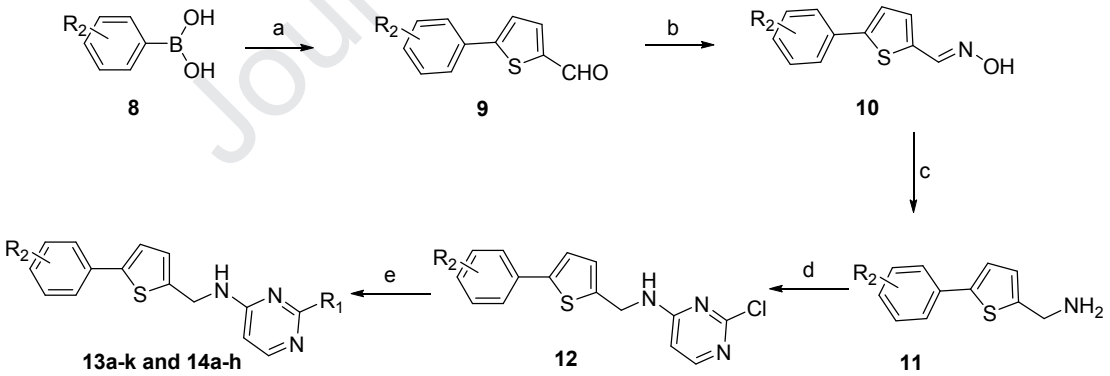


$R_1$ = i-Bu-NH- or Et-NH- or n-Pr-NH- or n-Bu-NH- or $(n\text{-Pr})_2$N- or $(n\text{-Bu})_2$N- or $(i\text{-Bu})_2$N- or pyrrolidinyl or piperazinyl or morpholinyl

$R_2$ = -H or -OBn or -OMe or -*t*-Bu or -F or -Cl or -Br

**Scheme 2**. Synthesis of compounds **13a-k** and **14a-h**. Reagents and conditions: (a) 5-bromo-2-thiophenecarboxaldehyde, $Pd(PPh_3)_4$, $Na_2CO_3$, EtOH, DME, 90 °C; (b)

$H_2$NOH-HCl, pyridine, EtOH, 80 °C; (c) Zn, AcOH; (d) 2,4-dichloropyrimidine, DIEA, EtOH, 40 °C; (e) appropriate amine, DIEA, n-BuOH, 120 °C.

## 3. Results and discussion

### *3.1. Structure-activity relationships against bacteria*

In this study, a series of phenylthiazole and phenylthiophene pyrimidindiamine derivatives were designed and synthesized. The MIC against Gram-negative bacteria *E. coli* and Gram-positive bacteria *S. aureus* was determined to evaluate their antibacterial efficacies and allowed us to rank their relative potencies. Initially, we shifted the diaminopyrimidinyl group from the 5'- to the 4'-position of the thiazole ring for investigating the best linking position of the diaminopyrimidinyl group and compounds **6** and **7** were synthesized. Regrettably, these compounds completely abolished their antibacterial activities compared to the hit compound, as shown in Table 1.

**Table 1**. MICs of compounds **6**, **7** against *E. coli* ATCC 25922 and *S. aureus* ATCC 29213.

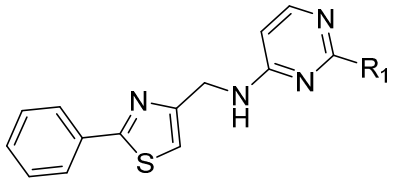


| Compd | $R_1$ | MIC (μg/mL) [α] | |
|---|---|---|---|
| | | *E. coli* | *S. aureus* |
| hit compound | - | 16 | 16 |
| **6** | Cl | >32 | >32 |
| **7** | i-Bu-NH- | >32 | >32 |
| **Vancomycin** | - | 1 | 4 |
| **Cefazolin** | - | 2 | 2 |
| **Chloromycetin** | - | 8 | 8 |

| | | | |
|---|---|---|---|
| **Polymyxin B** | - | 32 | 512 |
| **Chloramphenicol** | - | 8 | 8 |

[α]The MIC values were measured in two independent experiments with three replicates per experiment.

In order to improve the antibacterial activities of the hit compound, we replaced the thiazole ring of it with thiophene ring, and compound **13a** was synthesized. The results indicated the antibacterial activities of compound **13a** were increased compared with the hit compound (Table 2), which may suggest that the thiophene ring was more beneficial to sustain or enhance the antibacterial activities. To further explore the structure-activity relationship, compounds **13b-h** were synthesized by replacing isobutylamine of the pyrimidinyl-2-position of compound **13a** with other alkylamines. The results were shown in Table 2, compared with compound **13a**, the introduction of alkylamines group at the pyrimidinyl-2-position did not improve the antibacterial activities of the compounds. Nonetheless, the mono-substituted alkylaminopyrimidinyl might be more conducive to the maintenance of the antibacterial activities than corresponding bis-substituted derivatives (**13a** *vs* **13h** and **13c** *vs* **13f**). Similar results were also observed in the comparison **13e** with **13g**. Also, the role of heterocyclic groups was investigated (**13i-k**), unfortunately, the introduction of heterocyclic groups didn't enhance the antibacterial activities of compounds compared with **13a**, and substitutions with piperazinyl (**13j**) or morpholinyl (**13k**) almost completely deprived the antibacterial activities.

**Table 2**. MICs of compounds **13a-k** against *E. coli* ATCC 25922 and *S. aureus* ATCC 29213.

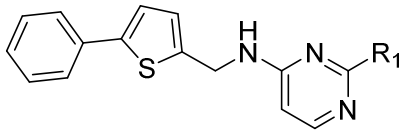

| Compd | $R_1$ | MIC (μg/mL) [α] | |
|---|---|---|---|
| | | *E. coli* | *S. aureus* |
| hit compound | - | 16 | 16 |
| **13a** | i-Bu-NH- | 8 | 8 |
| **13b** | Et-NH- | 16 | >32 |
| **13c** | n-Pr-NH- | 8 | 16 |
| **13d** | i-Pr-NH- | >32 | >32 |
| **13e** | n-Bu-NH- | >32 | 4 |
| **13f** | $(n\text{-Pr})_2N$- | 8 | >32 |
| **13g** | $(n\text{-Bu})_2N$- | >32 | >32 |
| **13h** | $(i\text{-Bu})_2N$- | >32 | >32 |
| **13i** | pyrrolidinyl | 8 | 8 |
| **13j** | piperazinyl | >32 | >32 |
| **13k** | morpholinyl | >32 | >32 |
| **Vancomycin** | - | 1 | 4 |
| **Cefazolin** | - | 2 | 2 |
| **Chloromycetin** | - | 8 | 8 |
| **Polymyxin B** | - | 32 | 512 |
| **Chloramphenicol** | - | 8 | 8 |

[α]The MIC values were measured in two independent experiments with three replicates per experiment.

Next, we focused the modification on the left part phenyl ring. As shown in Table 3, compared with the unsubstituted compound **13a**, the introduction of substituted groups to the phenyl ring was preferable for sustaining or enhancing the antibacterial activities. The derivatives with electron-donating substituents (**14a-c**) shared the similar antibacterial activities to the ones with electron-withdrawing substituents (**14d-h**), which may suggest that the electronic effect of this position has little influence on the antibacterial activities of compounds. Interestingly, the introduction of the fluorine substituent (**14d**) could effectively resist *S. aureus* with MIC value of 8

μg/mL, however, it didn't has any inhibitory activity against *E.coli* at the same concentration. In addition, the bromine group was introduced to different positions (*o*-, *m*- and *p*-position) of the phenyl ring (**14f-h**) to investigate the effect of the substitution position on antibacterial activity. As shown in Table 3, *m*-position substitution (**14g**) may be more favorable against both *E. coli* and *S. aureus* than *o*- or *p*-position (**14h** and **14f**), but it still needs more compounds to validate. Among the investigated compounds, compounds **14f** and **14g** exhibited the most excellent antibacterial activities with the MIC values of 2 μg/mL for *E. coli* and 3 or 4 μg/mL for *S. aureus*, which were comparable to or even better than the widely used positive controls vancomycin, cefazolin, chloromycetin, polymyxin B and chloramphenicol. Given compounds **14f** and **14g** shared very similar structures except of difference in the position of the bromine group, we speculated that their antibacterial activities and mechanism were also similar. Therefore, **14g** was selected as the representative compound for further research.

**Table 3**. MICs of compounds **14a-h** against *E. coli* ATCC 25922 and *S. aureus* ATCC 29213.

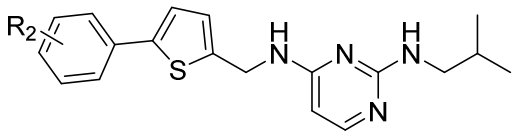


| Compd | $R_2$ | MIC (μg/mL) [α] | |
|---|---|---|---|
| | | *E. coli* | *S. aureus* |
| hit compound | - | 16 | 16 |
| **13a** | H | 8 | 8 |
| **14a** | 4-OBn | 8 | 8 |
| **14b** | 4-OMe | 4 | 4 |
| **14c** | 4-*t*-Bu | 2 | 8 |

| | | | |
|---|---|---|---|
| **14d** | 4-F | >32 | 8 |
| **14e** | 4-Cl | 8 | 8 |
| **14f** | 4-Br | 2 | 4 |
| **14g** | 3-Br | 2 | 3 |
| **14h** | 2-Br | 4 | 8 |
| **Vancomycin** | - | 1 | 4 |
| **Cefazolin** | - | 2 | 2 |
| **Chloromycetin** | - | 8 | 8 |
| **Polymyxin B** | - | 32 | 512 |
| **Chloramphenicol** | - | 8 | 8 |

[α]The MIC values were measured in two independent experiments with three replicates per experiment.

*3.2. Compound **14g** causes no significant hemolysis*

In order to determine whether compound **14g** is cytotoxic to mammalian cells, the hemolysis assays were performed using the rabbit's red blood cells. After exposure to different concentrations of compound **14g** for 1 h, hemolysis levels were below 20%, which indicated compound **14g** was not significantly hemolytic within its antibacterial activity range (Fig. 2) and suggested that compound **14g** could differentiate between microbial and erythrocyte cellular membrane. The difference between eukaryotic and prokaryotic cell membranes lies in the content and distribution of phospholipids [23, 29], which may contribute to the antibacterial activity of compound **14g**.

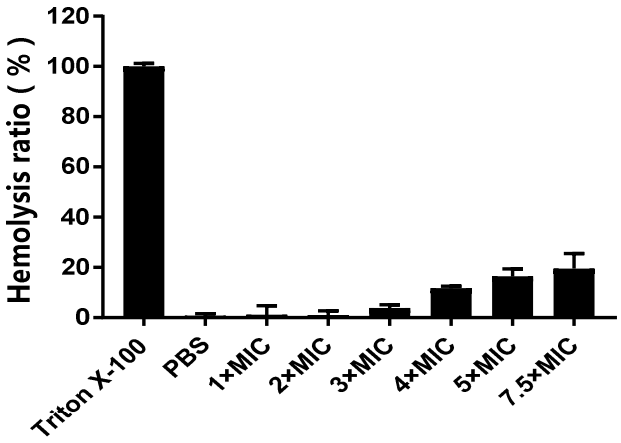

**Fig 2.** The hemolysis rate of rabbit red blood cell induced by positive control (Triton X-100), negative control (PBS) and **14g** at 1 ×, 2 ×, 3 ×, 4 ×, 5 ×, and 7.5 × MIC, respectively. Bars represent the standard deviation (n = 3).

*3.3. Compound **14g** inhibits bacterial growth*

To further determine the antibacterial efficacy of compound **14g** and how long it will start to exhibit the antibacterial effect, the effects of **14g** on the bacterial growth process were monitored at different concentrations. The results were recorded every two hours within 24 h, giving the complete growth cycle for bacteria. As shown in Fig. 3A-B, when the bacteria in the control group began to enter the logarithmic growth phase at the 6th hour of incubation, the growth of the bacteria was still wholly inhibited in the group treated with 1 × and 2 × MIC of compound **14g**. It suggested that the compound could exert an antibacterial effect within 6 h. Although 0.5 × MIC of compound **14g** showed little effects on the growths of *E. coli* and *S. aureus*, it still could delay the growth cycle of bacteria.

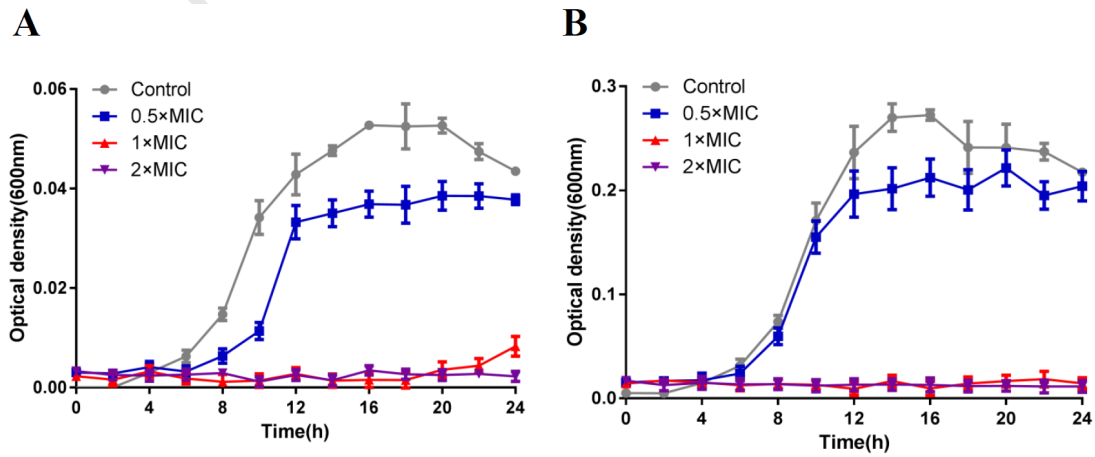


**Fig 3. (A)** Effect of **14g** on *E. coli* growth for 24 h. **(B)** Effect of **14g** on *S. aureus* growth for 24 h.

*3.4. Compound **14g** changes bacterial cell morphology*

The above results showed that compound **14g** could exert effect quickly within 6 h, possibly because it acted on the cell's first line of defense, the cell membrane, causing changes in cell morphology. To test whether the treatment of compound **14g** could change the cell morphology, Scanning Electron Microscopy (SEM) and Transmission Electron Microscopy (TEM) were performed.

As shown by SEM, a visible morphological change occurred on the surface of the treated strain compared to the untreated control. Untreated cells were regular, intact and had a smooth surface (Fig. 4A and 4C), while some bacterial cells treated with compound **14g** became deformed, pitted and shriveled. (Fig. 4B and 4D). TEM was used to intensify the investigation of the morphological changes of *E. coli* and *S. aureus.* Same as observed by SEM, the cell morphology of untreated bacteria was regular, the double membrane structure was smooth and continuous, and the cytoplasm was homogenous (Fig. 4E and 4G). In contrast, after treatment with compound **14g**, the entire cell shape was significantly modified or damaged, and the bacterial cells became ghost-like structures, resulting in electron density heterogeneity (Fig. 4F and 4H). The cell debris and electron-dense particles were found around the disrupted cells. The above results indicated that compound **14g** could destroy the cell membrane of *E. coli* and *S. aureus*.

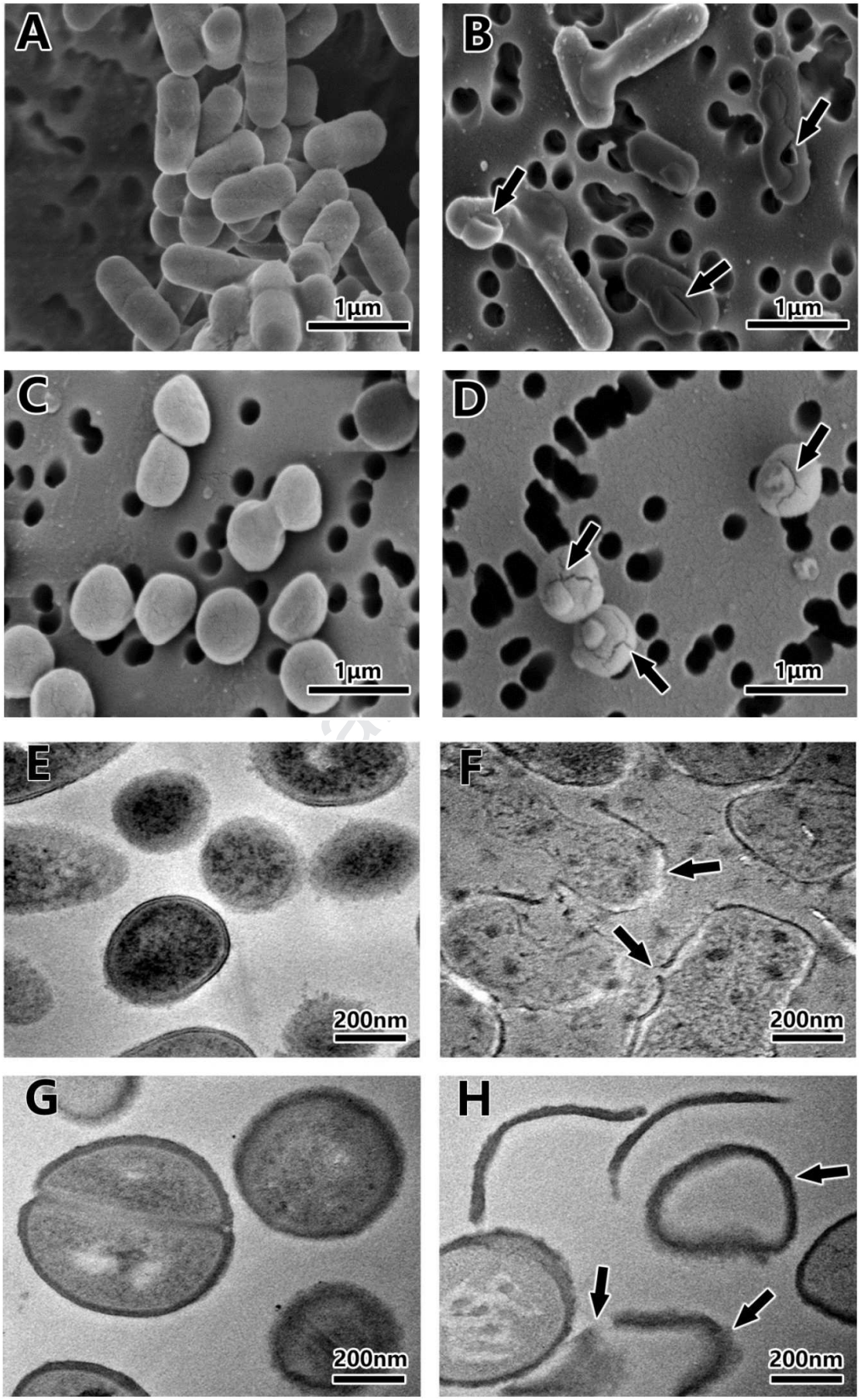
A
1µm
B
1µm
C
1µm
D
1µm
E
200nm
F
200nm
G
200nm
H
200nm

**Fig 4. (A-D)** Scanning electron microscopy images of *E. coli* and *S. aureus*. **(A)** Untreated *E. coli.* **(B)** *E. coli* treated with **14g** at 1 × MIC for 12 h. **(C)** Untreated *S. aureus.* **(D)** *S. aureus* treated with **14g** at 1 × MIC for 12 h. The black arrow indicates a rough cell membrane with some cracks and holes after treatment with **14g**. Bar = 1 μm. (**E-H**) Transmission electron microscopy images of *E. coli* and *S. aureus*. **(E)** Untreated *E. coli.* **(F)** *E. coli* treated with **14g** at 1 × MIC for 12 h. **(G)** Untreated *S. aureus*. **(H)** *S. aureus* treated with **14g** at 1 × MIC for 12 h. The black arrow indicates the leakage of intracellular contents, cell lysis and the appearance of ghost cells. Bar = 200 nm.

*3.5. Compound **14g** destroys bacteria membrane*

*3.5.1 Compound **14g** causes the leakage of cell contents*

To examine how the compound achieves antibacterial efficacy by altering the morphology of bacterial cells, changes in the physicochemical properties of the cell membrane after compound **14g** treatment were detected. The cell membrane is a vital component of bacteria, and it is responsible for providing a stable internal environment for the cells and for transporting materials or transmitting information function [30]. If the cell membranes are destroyed, the intracellular components, such as small ions, proteins and nucleotide will leak out. Therefore, the integrity of the cell membrane can be detected by some fluorescent stains of these components [31]. Ethidium bromide (EB) is an indicator of DNA structure. It binds nucleic acids via intercalative binding mode with changes in EB fluorescence [32]. When bacteria were exposed to compound **14g**, EB will be able to bind to the DNA released in culture or

damaged cells, causing an increase in fluorescence, in case compound **14g** could disrupt the bacterial membrane. As shown in Fig. 5A-B, compared to the solvent control group, the fluorescence of compound **14g** treatment groups significantly increased within 20 min, which indicated that compound **14g** could destroy the bacterial cell membranes. The red-fluorescent propidium iodide (PI), which can penetrate only membrane-broken cells and embed DNA to emit fluorescence, was used to further test the effects of compound **14g** on bacterial cell membranes. As shown in Fig. 5C-F, 77.16% of the compound **14g**-treated *E. coli* cells were stained by PI (Fig. 5D), while the stained cells only accounted for 4.34% in the solvent control group (Fig. 5C). The same result was also found in *S. aureus* group, the percentage of the damaged cells increased from 1.53% (Fig. 5E) to 58.47% after incubation with 1 × MIC compound **14g** for 1 h (Fig. 5F). The results showed that when exposed to compound **14g**, the integrity of the bacterial cell membranes was compromised and the contents leaked.

*3.5.2 Compound **14g** depolarizes bacterial cell membranes*

The structural damage of cell membranes often leads to potential variations in cell membranes [33]. The fluorescent probe $DiSC_3(5)$ can quench the fluorescence when inserted into a hyperpolarized membrane, and if the cell membranes are depolarized, it can be released to enhance the fluorescent signal. Therefore, the molecule $DiSC_3(5)$ was selected to detect changes in membrane potential caused by compound **14g**. As shown in Fig. 5G-H compound **14g** increased the fluorescence intensity in the co-incubation group compared to the solvent control or negative control vancomycin

in both *E. coli* and *S. aureus* group. The behavior was similar to that of the positive control of polymyxin B, which also produced an increase in fluorescence intensity. In the *S. aureus* group (Fig. 5H), the change in fluorescence intensity showed a more obvious dose-dependent manner and concentration-dependent characteristic. The results suggested that compound **14g** could dissipate the bacteria membrane potential.

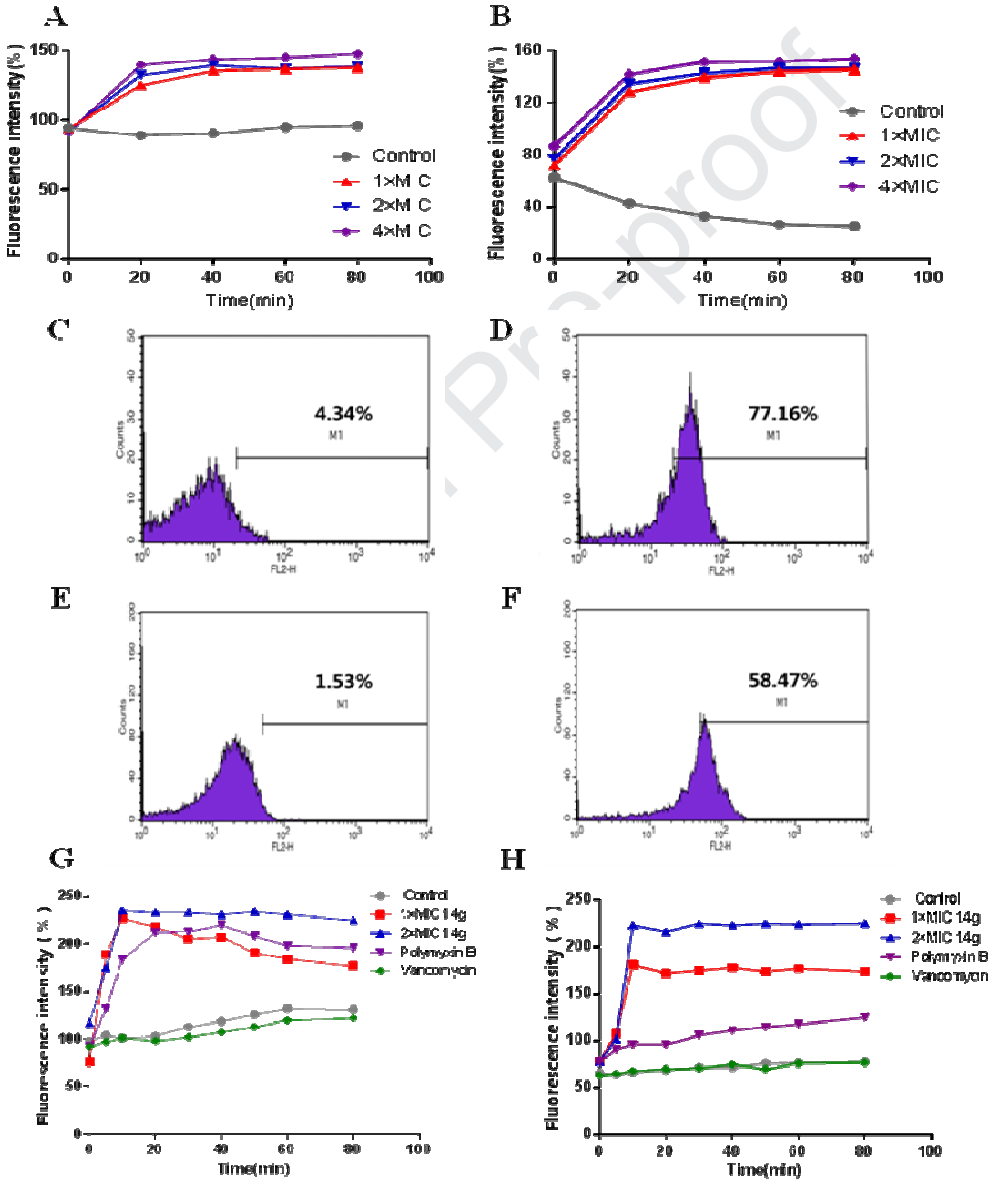


**Fig 5. (A-B)** Membrane disruption as measured by ethidium bromide uptake against **(A)** *E. coli* and **(B)** *S. aureus*. **(C-F)** FACScan analysis of PI staining in bacteria cells

treated with **14g** for 1 h. **(C)** Staining of *E. coli* cells without **14g** treatment. **(D)** Staining of *E. coli* cells treated with 1 × MIC **14g**. **(E)** Staining of *S. aureus* cells without **14g** treatment. **(F)** Staining of *S. aureus* cells treated with 1 × MIC **14g**. The percentage of PI-stained cells is indicated. M1 is the percentage of membrane disrupted cells. The x-axis shows the relative fluorescence intensity. The y-axis shows the relative number of cells. **(G-H)** Effect of **14g** on the membrane potential of bacterias. **(G)** *E. coli* treated with 1% DMSO, polymyxin B, vancomycin and **14g** at 1 × MIC, 2 × MIC for 80 min. **(H)** *S. aureus* treated with 1% DMSO, polymyxin B, vancomycin and **14g** at 1 × MIC, 2 × MIC for 80 min.

*3.6. Antibacterial activity of compound **14g** in vivo*

Encouraged by the excellent antibacterial activity of compound **14g** *in vitro*, the mouse bacteremia models infected by *S. aureus* were used to further assess the antibacterial activity of compound **14g** *in vivo*. It is known that murine models of bacteremia are commonly used to detect the systemic effects of antibiotics in the pharmaceutical industry [34]. The treatment was performed after the 1-hour injection, which is sufficient for the bacteria to spread throughout the mouse [35]. As shown in Fig. 6, compound **14g** could reduce the number of viable pathogens in the peritoneal cavity of infected mice at low dosage (12 mg/kg), but the efficacy was not as good as the same concentration of polymyxin B. The antibacterial efficacy of high dose compound **14g** (24 mg/kg) was better than polymyxin B. The results indicated that compound **14g** exhibited good antimicrobial activity *in vivo*.

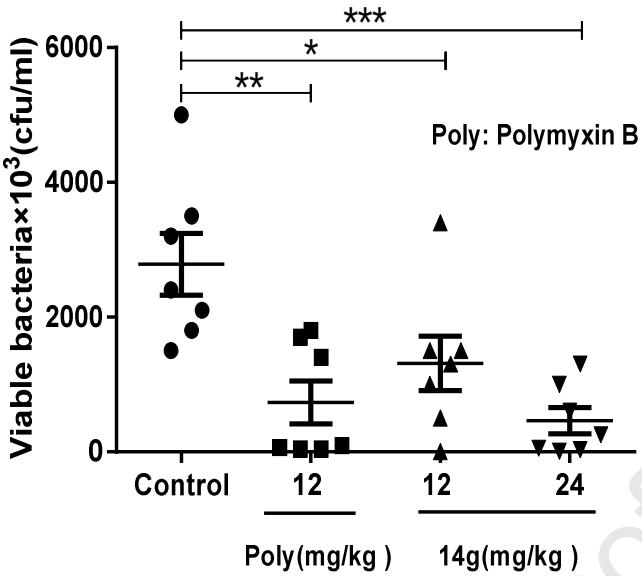


**Fig 6.** Viable bacterial counts of the abdominal cavity in the bacteremia model infected with *S. aureus* strain. The infected mice were treated with **14g** (12 and 24 mg/kg) or polymyxin B (12 mg/kg) via intraperitoneally injection (n = 7). Each point represents the determination of a single animal, and the line shows the mean value. *P < 0.05, **P < 0.01, ***P < 0.001, compared with untreated control group.

## 4. Conclusion

With the overuse and abuse of antibiotics, the problem of bacterial resistance has become more and more prominent, and new antibacterial agents are urgently needed to alleviate this situation [36, 37]. In this study, an in-house library was screened to discovery novel antibacterial candidates. The compound $N^2$-isobutyl-$N^4$-((4-methyl-2-phenylthiazol-5-yl)methyl)pyrimidine-2,4-diamine displayed mild antibacterial activity and presented as a hit compound. A series of phenylthiazole and phenylthiophene pyrimidindiamine derivatives with antibacterial potential were designed and synthesized by modifying the hit compound. Among the investigated compounds, compound **14g** showed the best antibacterial activities, which was not

only capable of inhibiting *E. coli* and *S. aureus in vitro*, but also was efficacious in a mice model of bacteremia *in vivo*. Moreover, further mechanism study revealed that compound **14g** plays an antibacterial role by inducing cytoplasmic membrane rupture, leading to the release of cell contents, and disordering membrane properties and functions, which can decrease the possibility of inducing bacterial resistance. Hence, compound **14g** is likely to be developed as a promising antibacterial candidate or to provide a kind of new chemical skeleton for the development of therapeutic agents.

## 5. Materials and methods

### *5.1. General methods for chemistry*

All reagents were purchased from Bide Pharmatech Ltd, Leyan Ltd. or Aladdin-reagents Inc.. Chemical reactions were completed through standard techniques under inert gas ($N_2$). Using Bruker 500 MHz instruments to generate NMR spectra. High-resolution mass spectra were collected on a Bruker MicroTOF-Q II LCMS instrument operating in electrospray ionization (ESI). The purity of the compounds was determined by high-pressure liquid chromatography (HPLC, Agilent Technologies 1200 Series) and the final purity of all biologically targeted compounds was ≥ 95%.

### *5.2. General procedure for the synthesis of compounds **6**, **7**, **13a-k** and **14a-h***

#### *5.2.1.* 2-Chloro-*N*-((2-phenyl-4-thiazolyl)methyl)-4-pyrimidinamine **(6)**.

Compound **6**, white solid (76% yield), was prepared according to our previous report [38], except using ethyl bromopyruvate instead of ethyl 2-chloroacetoacetate. $^1$H NMR (500 MHz, $CDCl_3$) $\delta$ 8.04 (d, $J$ = 1.1 Hz, 1H), 7.92 (dd, $J$ = 6.5, 3.2 Hz, 2H),

7.47 – 7.43 (m, 3H), 7.18 (s, 1H), 6.34 (d, *J* = 5.8 Hz, 1H), 4.70 (s, 2H). $^{13}$C NMR (125 MHz, $CDCl_3$) $\delta$ 169.08, 160.83, 152.75, 145.78, 133.20, 130.33, 129.01, 126.48, 115.39, 95.31, 29.67. HR MS (ESI): calcd for $C_{14}H_{11}ClN_4NaS$ $[M + Na]^+$; 325.0285; found 325.0295.

*5.2.2.* $N^2$-isobutyl-$N^4$-((2-phenyl-4-thiazolyl)methyl)pyrimidine-2,4-diamine (**7**).

A mix of compound **6** (70 mg, 0.23 mM) and isobutylamine (70 mg, 1.0 mM) in n-butyl alcohol (5 mL), then *N*,*N*-diisopropylethylamine (0.1 mL, 0.6 mM) was added. Then the mix was heated to 120 °C overnight. After reaction was completed, the solvent (n-butyl alcohol) was removed by evaporation and diluted with water, extracted with $CH_2Cl_2$. The $CH_2Cl_2$ layer was dried over anhydrous sodium sulfate, concentrated. The resulting crude product was purified by column chromatography ($CH_2Cl_2$/MeOH 100:1-20:1) to afford **7**, brown oily liquid (63 mg, 81%). $^1$H NMR (500 MHz, $CDCl_3$) $\delta$ 7.92 (dd, *J* = 6.6, 2.9 Hz, 2H), 7.53 (s, 1H), 7.47 – 7.42 (m, 3H), 7.16 (s, 1H), 5.92 (d, *J* = 5.7 Hz, 1H), 4.74 (s, 2H), 3.23 (t, *J* = 6.2 Hz, 2H), 1.92 – 1.84 (m, 1H), 0.95 (d, *J* = 6.7 Hz, 6H). $^{13}$C NMR (125 MHz, $CDCl_3$) $\delta$ 168.96, 162.57, 152.86, 146.06, 133.23, 130.31, 129.01, 126.48, 115.18, 95.30, 48.69, 41.72, 28.30, 20.24. HR MS (ESI): calcd for $C_{18}H_{22}N_5S$ $[M + H]^+$; 340.1590; found 340.1603.

*5.2.3.* $N^2$-isobutyl-$N^4$-((5-phenylthiophen-2-yl)methyl)pyrimidine-2,4-diamine **(13a)**.

A mix of compound 5-bromothiophene-2-carbaldehyde (1.55 mL, 13 mM) and catalytic tetrakis (triphenylphosphine) palladium in DME (20 mL), an aqueous solution of $Na_2CO_3$ (2.12 g in 10 mL of $H_2O$) was added at r.t, the vial was blown three times with $N_2$. After stirring for 5 min, compound phenylboronic acid (1.22 g,

10.0 mM) and EtOH (20 mL) were added, the resulting mix was degassed under vacuum and was heated to 90 °C overnight under $N_2$, then evaporated and extracted with $CH_2Cl_2$ and $H_2O$. The $CH_2Cl_2$ layer was dried over anhydrous sodium sulfate, concentrated. The residue was subjected to column chromatography (PE/EA = 20:1) to afford compound 5-phenylthiophene-2-carbaldehyde (1224 mg, 65%). A mix of compound 5-phenylthiophene-2-carbaldehyde (1224 mg, 6.5 mM) in anhydrous EtOH (40 mL), hydroxylamine hydrochloride (903 mg, 13 mM) and pyridine (1.05 mL, 13 mM) were added, then heated to 80 °C for 1 h, evaporated to afford crude 5-phenylthiophene-2-carbaldehyde oxime. To a solution of compound 5-phenylthiophene-2-carbaldehyde oxime in AcOH (10 mL), Zn (1.643 g, 25.13 mM) was added. The mix was stirred at r.t overnight. The resulting mix was filtered via a pad of Celite and the pad was washed with $CH_2Cl_2$ (15 mL × 3). After removal of the solvent by concentration, crude compound (5-phenyl-2-thiophenyl)methanamine was obtained. A mix of compound (5-phenyl-2-thiophenyl)methanamine (1041 mg, 5.5 mM) and 2,4-dichloropyrimidine (1639 mg, 11 mM) in anhydrous EtOH (50 mL), *N*,*N*-diisopropylethylamine (2.8 mL, 16.5 mM) was added, the mix was stirred at 40 °C overnight. Then the solvent was removed by evaporation and diluted with water, extracted with $CH_2Cl_2$. The $CH_2Cl_2$ layer was dried over anhydrous sodium sulfate, concentrated. The residue was subjected to column chromatography (PE/EA, 8:1-2:1) to obtain compound *N*-((5-phenyl-2-thiophenyl)-methyl)-2-chloropyrimidin-4-amine (1021 mg, 62%). A mix of compound *N*-((5-phenyl-2-thiophenyl)methyl)-2-chloro-pyrimidin-4-amine (60 mg, 0.2 mM) and isobutylamine (1.0 mL) in n-butyl alcohol (5

mL), *N*,*N*-diisopropylethylamine (0.1 mL, 0.6 mM) was added, and the resulting was stirred at 120 °C overnight. Then the solvent was removed by concentration and extracted with DCM and $H_2O$. The $CH_2Cl_2$ layer was dried over anhydrous sodium sulfate, concentrated. The residue was subjected to column chromatography ($CH_2Cl_2$/MeOH 100:1-20:1) to afford compound $N^2$-isobutyl-$N^4$-((5-phenylthiophen-2-yl)methyl)pyrimidine-2,4-diamine **13a**, light yellow solid (56 mg, 90%). $^1$H NMR (500 MHz, $CDCl_3$) $\delta$ 7.68 (d, $J$ = 7.4 Hz, 1H), 7.57 – 7.48 (m, 2H), 7.36 (dd, $J$ = 10.5, 4.8 Hz, 2H), 7.28 (d, $J$ = 7.4 Hz, 1H), 7.14 (d, $J$ = 3.6 Hz, 1H), 6.96 (d, $J$ = 3.6 Hz, 1H), 5.79 (d, $J$ = 6.2 Hz, 1H), 4.72 (d, $J$ = 4.1 Hz, 2H), 3.25 (t, $J$ = 6.3 Hz, 2H), 1.93 – 1.85 (m, 1H), 0.97 (d, $J$ = 6.7 Hz, 6H). $^{13}$C NMR (125 MHz, $CDCl_3$) $\delta$ 162.39, 144.06, 140.65, 134.16, 128.85, 127.50, 126.77, 125.61, 122.56, 95.29, 48.80, 40.00, 28.43, 20.24. HR MS (ESI): calcd for $C_{19}H_{23}N_4S$ $[M + H]^+$; 339.1638; found 339.1651.

*5.2.4.* $N^2$-ethyl-$N^4$-((5-phenylthiophen-2-yl)methyl)pyrimidine-2,4-diamine **(13b)**.

Similar procedures to the preparation of compound **13a** were used to synthesize compound **13b**, light yellow solid (90% yield), except using ethylamine replace with 2-methylpropanamine. $^1$H NMR (500 MHz, $CDCl_3$) $\delta$ 7.55 – 7.51 (m, 2H), 7.50 – 7.39 (m, 1H), 7.35 (t, $J$ = 7.6 Hz, 2H), 7.27 (d, $J$ = 7.4 Hz, 1H), 7.12 (d, $J$ = 3.6 Hz, 1H), 6.96 (d, $J$ = 3.6 Hz, 1H), 5.95 (d, $J$ = 5.6 Hz, 1H), 4.75 (d, $J$ = 4.4 Hz, 2H), 3.51 – 3.42 (m, 2H), 1.24 (t, $J$ = 7.2 Hz, 3H). $^{13}$C NMR (125 MHz, $CDCl_3$) $\delta$ 162.36, 144.16, 139.80, 134.04, 128.86, 127.55, 127.17, 125.57, 122.53, 96.40, 39.79, 36.14, 14.60. HR MS (ESI): calcd for $C_{17}H_{19}N_4S$ $[M + H]^+$; 311.1325; found 311.1339.

*5.2.5.* $N^4$-((5-phenylthiophen-2-yl)methyl)-$N^2$-propylpyrimidine-2,4-diamine **(13c)**.

Similar procedures to the preparation of compound **13a** were used to synthesize compound **13c**, light yellow solid (99% yield), except using propylamine replace with 2-methylpropanamine. $^{1}$H NMR (500 MHz, $CDCl_3$) $\delta$ 7.81 (d, $J$ = 4.4 Hz, 1H), 7.55 (d, $J$ = 7.8 Hz, 2H), 7.36 (t, $J$ = 7.6 Hz, 2H), 7.27 (d, $J$ = 7.7 Hz, 1H), 7.14 (d, $J$ = 3.6 Hz, 1H), 6.95 (d, $J$ = 3.5 Hz, 1H), 5.73 (d, $J$ = 5.8 Hz, 1H), 5.12 (s, 1H), 4.70 (d, $J$ = 5.0 Hz, 2H), 3.36 (dd, $J$ = 13.3, 6.6 Hz, 2H), 1.67 – 1.56 (m, 2H), 0.97 (t, $J$ = 7.4 Hz, 3H). $^{13}$C NMR (125 MHz, $CDCl_3$) $\delta$ 162.47, 144.02, 141.21, 134.25, 128.85, 127.48, 126.54, 125.67, 122.61, 94.59, 43.18, 40.14, 23.00, 11.51. HR MS (ESI): calcd for $C_{18}H_{21}N_4S$ $[M + H]^+$; 325.1481; found 325.1491.

*5.2.6.* $N^2$-isopropyl-$N^4$-((5-phenylthiophen-2-yl)methyl)pyrimidine-2,4-diamine **(13d)**.

Similar procedures to the preparation of compound **13a** were used to synthesize compound **13d**, light yellow solid (44% yield), except using isopropylamine replace with 2-methylpropanamine. $^{1}$H NMR (500 MHz, $CDCl_3$) $\delta$ 7.60 – 7.48 (m, 3H), 7.36 (t, $J$ = 7.6 Hz, 2H), 7.29 (d, $J$ = 7.5 Hz, 1H), 7.14 (d, $J$ = 3.6 Hz, 1H), 6.97 (d, $J$ = 3.5 Hz, 1H), 5.83 (d, $J$ = 6.5 Hz, 1H), 4.76 (d, $J$ = 3.9 Hz, 2H), 4.21 – 4.17 (m, 1H), 1.26 (d, $J$ = 6.5 Hz, 6H). $^{13}$C NMR (125 MHz, $CDCl_3$) $\delta$ 162.39, 144.28, 139.91, 134.08, 128.90, 127.60, 127.08, 125.63, 122.62, 94.95, 43.18, 39.98, 22.65. HR MS (ESI): calcd for $C_{18}H_{21}N_4S$ $[M + H]^+$; 325.1481; found 325.1495.

*5.2.7.* $N^2$-butyl-$N^4$-((5-phenylthiophen-2-yl)methyl)pyrimidine-2,4-diamine **(13e)**.

Similar procedures to the preparation of compound **13a** were used to synthesize compound **13e**, light yellow solid (44% yield), except using 1-butylamine replace

with 2-methylpropanamine. $^{1}$H NMR (500 MHz, $CDCl_3$) $\delta$ 7.53 (d, $J$ = 8.1 Hz, 2H), 7.36 (t, $J$ = 7.6 Hz, 2H), 7.27 (d, $J$ = 7.2 Hz, 1H), 7.13 (d, $J$ = 3.5 Hz, 1H), 6.96 (d, $J$ = 3.5 Hz, 1H), 5.87 (s, 1H), 4.74 (s, 2H), 3.43 (dd, $J$ = 12.7, 6.4 Hz, 2H), 1.64 – 1.55 (m, 2H), 1.46 – 1.36 (m, 2H), 0.92 (t, $J$ = 7.3 Hz, 3H). $^{13}$C NMR (125 MHz, $CDCl_3$) $\delta$ 162.38, 144.28, 139.89, 134.08, 128.88, 127.59, 127.08, 125.63, 122.57, 95.82, 41.03, 39.98, 31.50, 20.10, 13.80. HR MS (ESI): calcd for $C_{19}H_{23}N_4S$ $[M + H]^+$; 339.1638; found 339.1644.

*5.2.8.* $N^4$-((5-phenylthiophen-2-yl)methyl)-$N^2$,$N^2$-dipropylpyrimidine-2,4-diamine **(13f)**.

Similar procedures to the preparation of compound **13a** were used to synthesize compound **13f**, brown oily liquid (82% yield), except using dipropylamine replace with 2-methylpropanamine. $^{1}$H NMR (500 MHz, $CDCl_3$) $\delta$ 7.85 (d, $J$ = 6.0 Hz, 1H), 7.56 (d, $J$ = 7.5 Hz, 2H), 7.38 (t, $J$ = 7.7 Hz, 2H), 7.30 – 7.29 (m, 1H), 7.16 (d, $J$ = 3.6 Hz, 1H), 6.97 (d, $J$ = 3.6 Hz, 1H), 5.85 (d, $J$ = 5.3 Hz, 1H), 4.75 (d, $J$ = 5.7 Hz, 2H), 3.60 – 3.49 (m, 4H), 1.70 – 1.62 (m, 4H), 0.94 (t, $J$ = 7.4 Hz, 6H). $^{13}$C NMR (125 MHz, $CDCl_3$) $\delta$ 161.99, 143.78, 141.33, 140.05, 134.29, 128.84, 127.41, 126.44, 125.62, 122.59, 94.71, 49.73, 39.89, 21.06, 11.41. HR MS (ESI): calcd for $C_{21}H_{27}N_4S$ $[M + H]^+$; 367.1951; found 367.1967.

*5.2.9.* $N^2$,$N^2$-dibutyl-$N^4$-((5-phenylthiophen-2-yl)methyl)pyrimidine-2,4-diamine **(13g)**.

Similar procedures to the preparation of compound **13a** were used to synthesize compound **13g**, brown oily liquid (86% yield), except using dibutylamine replace

with 2-methylpropanamine. $^{1}$H NMR (500 MHz, $CDCl_3$) $\delta$ 7.91 (d, $J$ = 5.7 Hz, 1H), 7.57 (dd, $J$ = 8.1, 0.9 Hz, 2H), 7.37 (t, $J$ = 7.7 Hz, 2H), 7.29 – 7.27 (m, 1H), 7.16 (d, $J$ = 3.6 Hz, 1H), 6.95 (d, $J$ = 3.6 Hz, 1H), 5.67 (d, $J$ = 5.7 Hz, 1H), 4.90 (s, 1H), 4.74 (d, $J$ = 5.7 Hz, 2H), 3.57 – 3.49 (m, 4H), 1.63 ‑ 1.57 (m, 4H), 1.36 – 1.32 (m, 4H), 0.94 (t, $J$ = 5.8 Hz, 6H). $^{13}$C NMR (125 MHz, $CDCl_3$) $\delta$ 161.28, 156.12, 143.68, 142.13, 134.36, 128.81, 127.36, 126.15, 125.63, 122.55, 93.42, 60.38, 47.32, 30.20, 20.35, 14.08. HR MS (ESI): calcd for $C_{23}H_{31}N_4S$ $[M + H]^+$; 395.2264; found 395.2277.

*5.2.10.* $N^2$,$N^2$-diisobutyl-$N^4$-((5-phenylthiophen-2-yl)methyl)pyrimidine-2,4-diamine **(13h)**.

Similar procedures to the preparation of compound **13a** were used to synthesize compound **13h**, brown oily liquid (30% yield), except using diisobutylamine replace with 2-methylpropanamine. $^{1}$H NMR (500 MHz, $CDCl_3$) $\delta$ 7.88 (d, $J$ = 5.7 Hz, 1H), 7.55 (d, $J$ = 7.4 Hz, 2H), 7.36 (t, $J$ = 7.7 Hz, 2H), 7.27 – 7.26 (m, 1H), 7.14 (d, $J$ = 3.6 Hz, 1H), 6.94 (d, $J$ = 3.6 Hz, 1H), 5.65 (d, $J$ = 5.7 Hz, 1H), 4.81 (s, 1H), 4.71 (d, $J$ = 5.6 Hz, 2H), 3.39 (d, $J$ = 7.4 Hz, 4H), 2.19 – 2.10 (m, 2H), 0.88 (d, $J$ = 6.7 Hz, 12H). $^{13}$C NMR (125 MHz, $CDCl_3$) $\delta$ 161.83, 156.05, 143.73, 142.04, 134.38, 128.84, 127.39, 126.22, 125.65, 122.58, 93.01, 55.78, 40.02, 27.01, 20.36. HR MS (ESI): calcd for $C_{23}H_{31}N_4S$ $[M + H]^+$; 395.2264; found 395.2273.

*5.2.11. N*-((5-phenylthiophen-2-yl)methyl)-2-(1-pyrrolidinyl)pyrimidin-4-amine **(13i)**.

Similar procedures to the preparation of compound **13a** were used to synthesize compound **13i**, light yellow crystals (99% yield), except using pyrrolidine replace with 2-methylpropanamine. $^{1}$H NMR (500 MHz, $CDCl_3$) $\delta$ 7.90 (d, $J$ = 5.7 Hz, 1H),

7.55 (d, *J* = 7.8 Hz, 2H), 7.35 (t, *J* = 7.6 Hz, 2H), 7.27 – 7.26 (m, 1H), 7.14 (d, *J* = 3.5 Hz, 1H), 6.95 (d, *J* = 3.4 Hz, 1H), 5.70 (d, *J* = 5.8 Hz, 1H), 5.01 (s, 1H), 4.72 (d, *J* = 5.5 Hz, 2H), 3.57 (t, *J* = 6.4 Hz, 4H), 1.95 (t, *J* = 6.4 Hz, 4H). $^{13}$C NMR (125 MHz, $CDCl_3$) $\delta$ 162.09, 143.78, 141.78, 134.31, 128.80, 127.36, 126.42, 125.62, 122.51, 93.72, 46.47, 39.93, 25.48. HR MS (ESI): calcd for $C_{19}H_{21}N_4S$ $[M + H]^+$; 337.1481; found 337.1496.

*5.2.12. N*-((5-phenylthiophen-2-yl)methyl)-2-(1-piperazinyl)pyrimidin-4-amine **(13j)**.

Similar procedures to the preparation of compound **13a** were used to synthesize compound **13j**, brown crystals (64% yield), except using piperazine replace with 2-methylpropanamine. $^1$H NMR (500 MHz, $CDCl_3$) $\delta$ 7.90 (d, *J* = 5.7 Hz, 1H), 7.54 (d, *J* = 7.4 Hz, 2H), 7.36 (t, *J* = 7.7 Hz, 2H), 7.28 (s, 1H), 7.14 (d, *J* = 3.6 Hz, 1H), 6.94 (d, *J* = 3.5 Hz, 1H), 5.74 (d, *J* = 5.7 Hz, 1H), 4.99 (s, 1H), 4.70 (d, *J* = 5.6 Hz, 2H), 3.90 – 3.80 (m, 4H), 3.02 – 2.94 (m, 4H), 1.24 (d, *J* = 6.4 Hz, 1H). $^{13}$C NMR (125 MHz, $CDCl_3$) $\delta$ 161.31, 143.98, 141.35, 134.22, 128.85, 127.47, 126.48, 125.64, 122.54, 94.93, 51.61, 45.05, 43.58. HR MS (ESI): calcd for $C_{19}H_{22}N_5S$ $[M + H]^+$; 352.1590; found 352.1604.

*5.2.13.* 2-morpholino-*N*-((5-phenylthiophen-2-yl)methyl)pyrimidin-4-amine **(13k)**.

Similar procedures to the preparation of compound **13a** were used to synthesize compound **13k**, yellow solid (99% yield), except using morpholine replace with 2-methylpropanamine. $^1$H NMR (500 MHz, $CDCl_3$) $\delta$ 7.93 (d, *J* = 5.7 Hz, 1H), 7.59 – 7.54 (m, 2H), 7.38 (t, *J* = 7.7 Hz, 2H), 7.30 (d, *J* = 7.4 Hz, 1H), 7.16 (d, *J* = 3.6 Hz, 1H), 6.97 (d, *J* = 3.6 Hz, 1H), 5.78 (d, *J* = 5.7 Hz, 1H), 5.03 (s, 1H), 4.73 (d, *J* = 5.7

Hz, 2H), 3.83 – 3.80 (m, 4H), 3.79 – 3.77 (m, 4H). $^{13}$C NMR (125 MHz, $CDCl_3$) $\delta$ 161.54, 143.96, 141.39, 134.22, 128.85, 127.47, 126.47, 125.62, 122.52, 94.92, 66.91, 45.77, 44.29. HR MS (ESI): calcd for $C_{19}H_{21}N_4OS$ $[M + H]^+$; 353.1431; found 353.1440.

*5.2.14.* $N^4$-((5-(4-(benzyloxy)phenyl)thiophen-2-yl)methyl)-$N^2$-isobutylpyrimidine -2,4-diamine **(14a)**.

Similar procedures to the preparation of compound **13a** were used to synthesize compound **14a**, light yellow solid (94% yield), except using 4-benzyloxybenzeneboronic acid replace with phenylboronic acid. $^1$H NMR (500 MHz, DMSO-$d_6$) $\delta$ 7.68 (d, $J$ = 5.9 Hz, 1H), 7.51 (d, $J$ = 8.8 Hz, 2H), 7.46 (d, $J$ = 7.2 Hz, 2H), 7.40 (t, $J$ = 7.4 Hz, 2H), 7.33 (t, $J$ = 7.2 Hz, 1H), 7.20 (d, $J$ = 3.6 Hz, 1H), 7.04 (d, $J$ = 8.8 Hz, 2H), 6.98 (d, $J$ = 3.6 Hz, 1H), 5.83 (d, $J$ = 6.1 Hz, 1H), 5.13 (s, 2H), 4.64 (d, $J$ = 3.3 Hz, 2H), 3.11 – 3.05 (m, 2H), 1.89 – 1.80 (m, 1H), 0.88 (d, $J$ = 6.7 Hz, 6H). $^{13}$C NMR (125 MHz, DMSO-$d_6$) $\delta$ 158.29, 142.66, 137.40, 128.89, 128.31, 128.14, 127.30, 127.12, 126.86, 122.25, 115.82, 69.74, 48.64, 28.32, 20.69. HR MS (ESI): calcd for $C_{26}H_{29}N_4OS$ $[M + H]^+$; 444.2057; found 444.2053.

*5.2.15.* $N^2$-isobutyl-$N^4$-((5-(4-methoxyphenyl)thiophen-2-yl)methyl)pyrimidine-2,4 -diamine **(14b)**.

Similar procedures to the preparation of compound **13a** were used to synthesize compound **14b**, light yellow solid (65% yield), except using 4-methoxyphenylboronic acid replace with phenylboronic acid. $^1$H NMR (500 MHz, $CDCl_3$) $\delta$ 7.82 (d, $J$ = 4.8 Hz, 1H), 7.51 – 7.43 (m, 2H), 7.02 (d, $J$ = 3.6 Hz, 1H), 6.92 (d, $J$ = 3.6 Hz, 1H), 6.91

– 6.87 (m, 2H), 5.72 (d, *J* = 5.8 Hz, 1H), 4.99 (s, 1H), 4.67 (d, *J* = 5.2 Hz, 2H), 3.82 (s, 3H), 3.22 (t, *J* = 6.4 Hz, 2H), 1.92 – 1.83 (m, 1H), 0.96 (d, *J* = 6.7 Hz, 6H). $^{13}$C NMR (125 MHz, $CDCl_3$) $\delta$ 162.45, 162.17, 159.16, 143.94, 140.16, 127.14, 126.93, 126.46, 121.52, 114.24, 94.70, 55.32, 48. 92, 40.14, 28.50, 20.28. HR MS (ESI): calcd for $C_{20}H_{25}N_4OS$ $[M + H]^+$; 369.1744; found 369.1759.

*5.2.16.* $N^4$-((5-(4-(tert-butyl)phenyl)thiophen-2-yl)methyl)-$N^2$-isobutylpyrimidine-2,4 -diamine **(14c)**.

Similar procedures to the preparation of compound **13a** were used to synthesize compound **14c**, brown solid (48% yield), except using 4-tert-butylphenylboronic acid replace with phenylboronic acid. $^1$H NMR (500 MHz, $CDCl_3$) $\delta$ 7.84 (d, *J* = 5.1 Hz, 1H), 7.48 (d, *J* = 8.4 Hz, 2H), 7.38 (d, *J* = 8.4 Hz, 2H), 7.10 (d, *J* = 3.6 Hz, 1H), 6.93 (d, *J* = 3.5 Hz, 1H), 5.73 (d, *J* = 5.8 Hz, 1H), 4.97 (s, 1H), 4.68 (d, *J* = 5.2 Hz, 2H), 3.22 (t, *J* = 6.4 Hz, 2H), 1.90 – 1.85 (m, 1H), 1.33 (s, 9H), 0.96 (d, *J* = 6.7 Hz, 6H). $^{13}$C NMR (125 MHz, $CDCl_3$) $\delta$ 162.40, 156.30, 150.58, 144.02, 140.77, 131.51, 126.42, 125.75, 125.41, 122.17, 94.71, 48.94, 40.15, 34.56, 31.23, 28.51, 20.29. HR MS (ESI): calcd for $C_{23}H_{31}N_4S$ $[M + H]^+$; 395.2264; found 395.2277.

*5.2.17.* $N^4$-((5-(4-fluorophenyl)thiophen-2-yl)methyl)-$N^2$-isobutylpyrimidine-2,4 -diamine **(14d)**.

Similar procedures to the preparation of compound **13a** were used to synthesize compound **14d**, light yellow solid (98% yield), except using 4-fluorobenzeneboronic acid replace with phenylboronic acid. $^1$H NMR (500 MHz, $CDCl_3$) $\delta$ 7.48 (dd, *J* = 8.6, 5.3 Hz, 3H), 7.05 (dd, *J* = 9.9, 7.2 Hz, 3H), 6.95 (d, *J* = 3.5 Hz, 1H), 5.95 (s, 1H),

4.75 (s, 2H), 3.27 (t, *J* = 6.2 Hz, 2H), 1.94 – 1.86 (m, 1H), 0.97 (d, *J* = 6.7 Hz, 6H). $^{13}$C NMR (125 MHz, $CDCl_3$) $\delta$ 163.28, 162.35, 161.32, 143.12, 130.38, 127.29, 122.57, 115.94, 115.77, 95.61, 48.68, 39.86, 28.37, 20.23. HR MS (ESI): calcd for $C_{19}H_{22}FN_4S$ $[M + H]^+$; 357.1544; found 357.1555.

*5.2.18.* $N^4$-((5-(4-chlorophenyl)thiophen-2-yl)methyl)-$N^2$-isobutylpyrimidine-2,4 -diamine **(14e)**.

Similar procedures to the preparation of compound **13a** were used to synthesize compound **14e**, brown solid (94% yield), except using 4-chlorobenzeneboronic acid replace with phenylboronic acid. $^1$H NMR (500 MHz, $CDCl_3$) $\delta$7.55 – 7.41 (m, 3H), 7.32 (d, *J* = 8.3 Hz, 2H), 7.11 (d, *J* = 3.2 Hz, 1H), 6.97 (d, *J* = 3.4 Hz, 1H), 5.93 (s, 1H), 4.75 (s, 2H), 3.27 (t, *J* = 5.9 Hz, 2H), 1.93 – 1.87 (m, 1H), 0.97 (d, *J* = 6.7 Hz, 6H). $^{13}$C NMR (125 MHz, DMSO-$d_6$) $\delta$ 162.02, 156.01, 145.61, 141.01, 132.64, 131.88, 129.04, 127.34, 126.72, 123.78, 96.20, 47.90, 31.14, 27.79, 20.06. HR MS (ESI): calcd for $C_{19}H_{22}ClN_4S$ $[M + H]^+$; 373.1248; found 373.1257.

*5.2.19.* $N^4$-((5-(4-bromophenyl)thiophen-2-yl)methyl)-$N^2$-isobutylpyrimidine-2,4 -diamine **(14f)**.

Similar procedures to the preparation of compound **13a** were used to synthesize compound **14f**, brown solid (83% yield), except using 4-bromophenylboronic acid replace with phenylboronic acid. $^1$H NMR (500 MHz, DMSO-$d_6$) $\delta$ 7.67 (d, *J* = 5.8 Hz, 1H), 7.57 (d, *J* = 8.2 Hz, 2H), 7.53 (d, *J* = 8.5 Hz, 2H), 7.38 (d, *J* = 3.1 Hz, 1H), 7.02 (d, *J* = 3.1 Hz, 1H), 5.81 (d, *J* = 5.9 Hz, 1H), 4.64 (d, *J* = 2.7 Hz, 2H), 3.08 (s, 2H), 1.90 – 1.73 (m, 1H), 0.86 (d, *J* = 6.5 Hz, 6H). $^{13}$C NMR (125 MHz, $CDCl_3$) $\delta$

162.37, 142.16, 141.31, 136.14, 130.33, 128.41, 127.00, 124.13, 123.37, 122.94, 96.11, 48.72, 39.83, 28.40, 20.22. HR MS (ESI): calcd for $C_{19}H_{22}BrN_4S$ $[M + H]^+$; 417.0743; found 417.0759.

*5.2.20.* $N^4$-((5-(3-bromophenyl)thiophen-2-yl)methyl)-$N^2$-isobutylpyrimidine-2,4 -diamine **(14g)**.

Similar procedures to the preparation of compound **13a** were used to synthesize compound **14g**, brown solid (78% yield), except using 3-bromophenylboronic acid replace with phenylboronic acid. $^1$H NMR (500 MHz, DMSO-$d_6$) $\delta$ 7.77 (t, $J$ = 1.7 Hz, 1H), 7.69 (d, $J$ = 6.2 Hz, 1H), 7.58 (d, $J$ = 7.9 Hz, 1H), 7.46 (t, $J$ = 7.2 Hz, 2H), 7.35 (d, $J$ = 7.9 Hz, 1H), 7.04 (d, $J$ = 3.6 Hz, 1H), 5.87 (d, $J$ = 5.9 Hz, 1H), 4.67 (d, $J$ = 3.6 Hz, 2H), 3.13 (d, $J$ = 0.8 Hz, 2H), 1.90 – 1.80 (m, 1H), 0.88 (d, $J$ = 6.7 Hz, 6H). $^{13}$C NMR (125 MHz, $CDCl_3$) $\delta$ 162.37, 142.16, 141.23, 136.14, 130.33, 128.41, 127.00, 124.13, 123.37, 122.94, 95.87, 48.72, 39.83, 28.40, 20.22. HR MS (ESI): calcd for $C_{19}H_{22}BrN_4S$ $[M + H]^+$; 417.0743; found 417.0738.

*5.2.21.* $N^4$-((5-(2-bromophenyl)thiophen-2-yl)methyl)-$N^2$-isobutylpyrimidine-2,4 -diamine **(14h)**.

Similar procedures to the preparation of compound **13a** were used to synthesize compound **14h**, brown solid (88% yield), except using 2-bromophenylboronic acid replace with phenylboronic acid. $^1$H NMR (500 MHz, DMSO-$d_6$) $\delta$ 7.74 (d, $J$ = 7.4 Hz, 1H), 7.69 (d, $J$ = 6.2 Hz, 1H), 7.50 (dd, $J$ = 7.7, 1.4 Hz, 1H), 7.47 – 7.40 (m, 1H), 7.30 – 7.27 (m, 1H), 7.19 (d, $J$ = 3.6 Hz, 1H), 7.06 (d, $J$ = 3.5 Hz, 1H), 5.90 (d, $J$ = 5.7 Hz, 1H), 4.71 (d, $J$ = 2.6 Hz, 2H), 3.21 – 3.03 (m, 2H), 1.88 – 1.80 (m, 1H), 0.87

(d, $J$ = 6.7 Hz, 6H). $^{13}$C NMR (125 MHz, DMSO-$d_6$) $\delta$ 162.02, 139.78, 134.49, 133.63, 131.68, 129.60, 128.10, 127.51, 125.91, 121.49, 94.86, 47.83, 31.31, 27.79, 20.14. HR MS (ESI): calcd for $C_{19}H_{22}BrN_4S$ $[M + H]^+$; 417.0743; found 417.0759.

*5.3. Biological evaluation*

*5.3.1. Bacterial strains*

The bacterial strains used in this study including Gram-negative bacteria *Escherichia coli* ATCC 25922 (*E. coli*) and Gram-positive bacteria *Staphylococcus aureus* ATCC 29213 (*S. aureus*) were stored at -80 °C in glycerol (20%, v/v) until used. All bacterial strains were incubated in Mueller Hinton broth (MHB) at 37 °C with constant shaking overnight.

*5.3.2. Animals*

Male C57BL/6 mice weighing 20 ± 2 g were purchased from the Shanghai Laboratory Animal Company, kept under pathogen-free conditions by institutional guidelines. All the experimental protocols have been approved by the Animal Investigation Committee of East China Normal University.

*5.3.3. Measurement of minimum inhibitory concentration (MIC)*

According to the guidelines of Clinical & Laboratory Standards Institute (CLSI), the minimal inhibitory concentration (MIC) of each compound was determined as the lowest concentration to restrain the growth of bacteria by the broth micro-dilution assay [39]. A 100 μL culture containing approximately $10^6$ CFU/mL bacteria (*E. coli* and *S. aureus*) and the same volume of the compound at different concentrations were added to each well of a 96-well plate. The final concentrations ranged from 1 to

32 μg/mL. The plate was then incubated at 37 °C for 24 h and the optical density at 600 nm (OD600) was measured.

*5.3.4. Hemolysis assays*

After washing and resuspending in PBS, 2% of rabbit erythrocyte solution was added to a 96-well plate with 100 μL per well. Then the same volume of compound **14g** in various concentrations was added. The final concentrations ranged from 3 (1 × MIC to *S. aureus*) to 22.5 (7.5 × MIC to *S. aureus*) μg/mL. 0.5% Triton X-100 (v:v) and PBS were used as positive control and negative control, respectively. After co-incubation at room temperature for one hour, the plate was centrifuged at 1500 rpm for 10 min. The absorbance of 100 μL of the supernatant was measured at 450 nm. The experiments were performed in triplicate, and the hemolysis percentage was calculated as follows: Hemolysis (%) = (A14g – APBS) / (ATriton – APBS) × 100%.

*5.3.5. Growth curves*

To detect when the compound exhibited activity and its effect on bacterial growth, a slightly modified method was used [40]. Briefly, the bacteria in the MHB media were treated with **14g** at different concentrations and gently shaken at 37 °C for 24 h (220 rpm). Except for the absence of **14g**, the bacterial culture was incubated with 1% DMSO under the same conditions as the solvent control of treatment.

*5.3.6. Morphology of the bacteria*

Scanning Electron Microscopy (SEM) analysis and Transmission Electron Microscopy (TEM) analysis were performed to investigate the morphology and ultrastructure alteration of the *E. coli* and *S. aureus* under the compound treatment.

*5.3.6.1. Preparation of samples*

*E. coli* and *S. aureus* were collected by centrifugation and washed thrice with phosphate buffer saline (PBS) following 8 h treatment with 1 × MIC **14g** or PBS as the treated group and control group, respectively.

*5.3.6.2. Scanning Electron Microscopy analysis*

The SEM analysis was researched according to a modified method described [41]. The precipitates were put in a chamber made of the 0.2 μm Isopore Membrane (Millipore, GTTP 04700) and sealed with the Parafilm (Parafilm, PM996). The chambers were fixed in 2.5% glutaraldehyde for 2 h, washed thrice with PBS, dehydrated with a series of ethanol solutions, dried with a critical point dryer (Leica EM CPD 300, Leica Microsystems GmbH, Wetzlar, Germany), and sprayed with gold in an ion coater (ACE600, Leica Microsystems). The prepared samples were observed using a scanning electron microscope (Hitachi S-4800, Japan) at an accelerating voltage of 3 kV.

*5.3.6.3. Transmission electron microscopy analysis*

The TEM analysis was researched according to a modified method described [42, 43]. The cell precipitates were fixed with 2.5% glutaraldehyde and 1% osmium tetraoxide for 2 h, respectively. After each fixation, the samples were washed thrice with PBS. Then the samples were dehydrated with a series of acetones and embedded in Eponate 12 (Ted Pella) resin. After ultrathin sectioning, the samples were observed with a transmission electron microscope (Hitachi HT7700, Japan) at an accelerating voltage of 100 kV.

*5.3.7. Cell Integrity*

*5.3.7.1. Ethidium bromide uptake assay*

The experimental process was adapted from previous work [44, 45]. After centrifugation and washing, the cells in the logarithmic growth phase were resuspended in PBS and diluted to contain approximately $10^8$ CFU/mL bacteria. The 30 μL of EB (10 mM final concentration) and the same volume of **14g** at various concentrations were added to 540 μL of the suspension. The fluorescence intensity was investigated by a fluorescence spectrophotometer (Hitachi F-4500, Japan) every 20 min for 80 min (excitation = 540 nm, emission = 590 nm).

*5.3.7.2. Flow cytometric analysis*

The effect of compound **14g** on the membrane integrity of *E. coli* and *S. aureus* was further evaluated using propidium iodide (PI) by protocol adapted from previous work[46]. The logarithmic phase bacterial cells were diluted to approximately $10^9$ CFU/mL with PBS and then exposed to 1 × MIC **14g** at 37 °C for 1 h. After centrifugation, washing and resuspension, the cells were stained with 60 μM PI in the dark for 15 min. Then the cell suspensions were immediately analyzed by a cell flow cytometer (BD FACSCalibur $^{TM}$). The sample treated without **14g** was used as negative control.

*5.3.8. Membrane depolarization study*

According to previous reports, 3,3'-dipropylthiadicarbocyanine iodide ($DiSC_3(5)$) was used to investigate membrane depolarization [44, 47, 48]. Depolarization of a membrane can be visualized by an increase in fluorescence. The logarithmic bacterial

cells were diluted to $10^7$ CFU/mL in PBS containing 0.4 μM $DiSC_3(5)$ and 0.1 M KCl in darkness. After addition of the different concentrations of **14g**, polymyxin B (positive control), vancomycin (negative control), 1% DMSO to the suspension, the changes in fluorescence intensity in the system were continuously recorded using a fluorescence spectrophotometer (Hitachi F-4500, Japan) for 80 min (excitation = 622 nm, emission = 670 nm).

*5.3.9. In vivo antibacterial activity assay*

The infection model of bacteremia was established according to a modified method described [49]. The mid-log phase *S. aureus* was centrifuged and washed, then diluted and resuspended in sterile saline to obtain the required CFU of bacteria for infection. C57BL/6 mice (20 ± 2 g) were injected intraperitoneally of a 200 μL of the suspension (about $10^9$ CFU per 20 g body weight). Then mice were treated intraperitoneally with 12 mg/kg, 24 mg/kg of **14g**, 0.9% sterile saline (control group) and 12 mg/kg polymyxin B (positive control group) at 1 h after injection (7 mice per group). After 24 h, *S. aureus* was obtained from the abdominal cavity of each mouse by lavage with 2 mL PBS. Then the 10-fold serial dilution of bacterial suspension was added to Tryptic Soy Agar (TSA) plates. The plates were incubated at 37 °C for 18-24 h. Single CFU was counted to determine *S. aureus* number in peritoneal fluid.

*5.4. Statistical analysis*

The data were expressed as mean ± standard deviation (SD) of triplicate experiments. First, one-way ANOVA was used to calculate the statistical difference among more than two groups. Then the Student's-test procedures were further

conducted to assess the significant difference between each of the two groups. The differences was considered significant when $P < 0.05$(*), $P < 0.01$(**) or $P < 0.001$(***).

**Notes**

The authors declare no conflicts of interest.

**Acknowledgments**

The work was supported by the grants from National Key R&D Program of China [2018YFA0507000]; National Natural Science Foundation of China [81773204, 81673304 and 81973160]; Innovation Program of Shanghai Municipal Education Commission [2017-01-07-00-05-E00011], Shenzhen Municipal Government of China [KQTD20170810160226082], Shanghai Natural Science Foundation [18ZR1431700], and ECNU Public Platform for Innovation [011].

**References**

[1] S.B. Singh, J.F. Barrett, Empirical antibacterial drug discovery--foundation in natural products, Biochem. Pharmacol., 71 (2006) 1006-1015.
[2] B. Wang, B. Pachaiyappan, J.D. Gruber, M.G. Schmidt, Y.M. Zhang, P.M. Woster, Antibacterial Diamines Targeting Bacterial Membranes, J. Med. Chem., 59 (2016) 3140-3151.
[3] R. Laxminarayan, P. Matsoso, S. Pant, C. Brower, J.A. Rottingen, K. Klugman, S. Davies, Access to effective antimicrobials: a worldwide challenge, Lancet (London, England), 387 (2016) 168-175.
[4] Y. Qu, J. Xu, H. Zhou, R. Dong, M. Kang, J. Zhao, Chitin Oligosaccharide (COS) Reduces Antibiotics Dose and Prevents Antibiotics-Caused Side Effects in Adolescent Idiopathic Scoliosis (AIS) Patients with Spinal Fusion Surgery, Marine Drugs, 15 (2017) 70.
[5] R. Laxminarayan, A. Duse, C. Wattal, A.K. Zaidi, H.F. Wertheim, N. Sumpradit, E. Vlieghe, G.L. Hara, I.M. Gould, H. Goossens, C. Greko, A.D. So, M. Bigdeli, G. Tomson, W. Woodhouse, E. Ombaka, A.Q. Peralta, F.N. Qamar, F. Mir, S. Kariuki, Z.A. Bhutta, A. Coates, R. Bergstrom, G.D. Wright, E.D. Brown, O. Cars, Antibiotic resistance-the need for global solutions, The Lancet Infectious diseases, 13 (2013) 1057-1098.
[6] V.M. D'Costa, C.E. King, L. Kalan, M. Morar, W.W. Sung, C. Schwarz, D. Froese,

G. Zazula, F. Calmels, R. Debruyne, G.B. Golding, H.N. Poinar, G.D. Wright, Antibiotic resistance is ancient, Nature, 477 (2011) 457-461.
[7] C. Anthony, H. Yanmin, B. Richard, P. Clive, The future challenges facing the development of new antimicrobial drugs, Nat. Rev. Drug Discov., 1 (2002) 895-910.
[8] A.M. Matallah, L. Bouayad, S. Boudjellaba, F. Mebkhout, T.M. Hamdi, N. Ramdani-Bouguessa, Staphylococcus aureus isolated from selected dairies of Algeria: Prevalence and susceptibility to antibiotics, Vet. World, 12 (2019) 205-210.
[9] I. Martin, P. Sawatzky, V. Allen, B. Lefebvre, L. Hoang, P. Naidu, J. Minion, P. Van Caeseele, D. Haldane, R.R. Gad, G. Zahariadis, A. Corriveau, G. German, K. Tomas, M.R. Mulvey, Multidrug-resistant and extensively drug-resistant Neisseria gonorrhoeae in Canada, 2012-2016, Can. Commun. Dis. Rep., 45 (2019) 45-53.
[10] K.M.M. Parnanen, C. Narciso-da-Rocha, D. Kneis, T.U. Berendonk, D. Cacace, T.T. Do, C. Elpers, D. Fatta-Kassinos, I. Henriques, T. Jaeger, A. Karkman, J.L. Martinez, S.G. Michael, I. Michael-Kordatou, K. O'Sullivan, S. Rodriguez-Mozaz, T. Schwartz, H. Sheng, H. Sorum, R.D. Stedtfeld, J.M. Tiedje, S.V.D. Giustina, F. Walsh, I. Vaz-Moreira, M. Virta, C.M. Manaia, Antibiotic resistance in European wastewater treatment plants mirrors the pattern of clinical antibiotic resistance prevalence, Sci. Adv., 5 (2019) eaau9124.
[11] H. Chen, L. Jing, Z. Yao, F. Meng, Y. Teng, Prevalence, source and risk of antibiotic resistance genes in the sediments of Lake Tai (China) deciphered by metagenomic assembly: A comparison with other global lakes, Environ. Int., 127 (2019) 267-275.
[12] P. Vikesland, E. Garner, S. Gupta, S. Kang, A. Maile-Moskowitz, N. Zhu, Differential Drivers of Antimicrobial Resistance across the World, Acc. Chem. Res., 52 (2019) 916-924.
[13] J. O'NEILL, Tackling drug-resistant infections globally: final report and recommendations, The review on antimicrobial resistance, (2016).
[14] U.D.o. Health, H. Services, Antibiotic resistance threats in the United States, 2013, (2013).
[15] C. Pillar, D. Sahm, Resistance Trends and Susceptibility Profiles in the US Among Prevalent Clinical Pathogens: Lessons from Surveillance, in Springer US, 2012, pp. 753-792.
[16] M.S. Butler, M.A. Blaskovich, M.A. Cooper, Antibiotics in the clinical pipeline at the end of 2015, The Journal of antibiotics, 70 (2017) 3-24.
[17] R. Gleckman, N. Blagg, D.W. Joubert, Trimethoprim: mechanisms of action, antimicrobial activity, bacterial resistance, pharmacokinetics, adverse reactions, and therapeutic indications, Pharmacotherapy, 1 (1981) 14-20.
[18] W.J. Suling, L.E. Seitz, V. Pathak, L. Westbrook, E.W. Barrow, S. Zywno-Van-Ginkel, R.C. Reynolds, J.R. Piper, W.W. Barrow, Antimycobacterial activities of 2,4-diamino-5-deazapteridine derivatives and effects on mycobacterial dihydrofolate reductase, Antimicrob. Agents Chemother., 44 (2000) 2784-2793.
[19] J.M. Beierlein, K.M. Frey, D.B. Bolstad, P.M. Pelphrey, T.M. Joska, A.E. Smith, N.D. Priestley, D.L. Wright, A.C. Anderson, Synthetic and crystallographic studies of a new inhibitor series targeting Bacillus anthracis dihydrofolate reductase, J. Med.

Chem., 51 (2008) 7532-7540.
[20] B. Nammalwar, R.A. Bunce, K.D. Berlin, C.R. Bourne, P.C. Bourne, E.W. Barrow, W.W. Barrow, Synthesis and biological activity of substituted 2,4-diaminopyrimidines that inhibit Bacillus anthracis, Eur. J. Med. Chem., 54 (2012) 387-396.
[21] L. Su, J. Li, Z. Zhou, D. Huang, Y. Zhang, H. Pei, W. Guo, H. Wu, X. Wang, M. Liu, C.-G. Yang, Y. Chen, Design, synthesis and evaluation of hybrid of tetrahydrocarbazole with 2,4-diaminopyrimidine scaffold as antibacterial agents, Eur. J. Med. Chem., 162 (2019) 203-211.
[22] K. Kupferschmidt, Resistance fighters, Science, 352 (2016) 758-761.
[23] Z. Michael, Antimicrobial peptides of multicellular organisms, Nature, 415 (2002) 389-395.
[24] N. Zhang, S. Ma, Recent development of membrane-active molecules as antibacterial agents, Eur. J. Med. Chem., 184 (2019) 111743.
[25] J. Jimenez-Barbero, F.J. Canada, S. Martin-Santamaria, [RSC Drug Discovery] Carbohydrates in Drug Design and Discovery || Chapter 11. Amphiphilic Aminoglycoside Antimicrobials in Antibacterial Discovery, 10.1039/9781849739993 255-285.
[26] J.G. Hurdle, A.J. O'Neill, I. Chopra, R.E. Lee, Targeting bacterial membrane function: an underexploited mechanism for treating persistent infections, Nat. Rev. Microbiol., 9 (2011) 62-75.
[27] M. Wenzel, A.I. Chiriac, A. Otto, D. Zweytick, J.E. Bandow, Small cationic antimicrobial peptides delocalize peripheral membrane proteins, Proc. Nat.l Acad. Sci. USA., 111 (2014) E1409.
[28] Z. Louis, K. Julie, B. Florian, S. Jitendriya, M.-L. Marie-Paule, D. Jean-Luc, Broad-spectrum antibacterial amphiphilic aminoglycosides: A new focus on the structure of the lipophilic groups extends the series of active dialkyl neamines, Eur. J. Med. Chem., 157 (2018) 1512-1525.
[29] J.L. Shu, N.M. O'Briensimpson, N. Pantarat, A. Sulistio, E.H.H. Wong, Y.Y. Chen, J.C. Lenzo, J.A. Holden, A. Blencowe, E.C. Reynolds, Combating multidrug-resistant Gram-negative bacteria with structurally nanoengineered antimicrobial peptide polymers, Nature Microbiology, 1 (2016) 16162.
[30] S. Matsuoka, Physiological function of membrane lipids and cell surface structure in bacteria, Genes & Genetic Systems, 92 (2017) 215-215.
[31] H. Chen, B. Wang, D. Gao, M. Guan, L. Zheng, H. Ouyang, Z. Chai, Y. Zhao, W. Feng, Broad-Spectrum Antibacterial Activity of Carbon Nanotubes to Human Gut Bacteria, Small, 9 (2013) 2735-2746.
[32] V.A. Izumrudov, M.V. Zhiryakova, A.A. Goulko, Ethidium Bromide as a Promising Probe for Studying DNA Interaction with Cationic Amphiphiles and Stability of the Resulting Complexes, Langmuir, 18 (2002) 10348-10356.
[33] J. Cho, H. Choi, J. Lee, M.-S. Kim, H.-Y. Sohn, D.G. Lee, The antifungal activity and membrane-disruptive action of dioscin extracted from Dioscorea nipponica, Biochimica et Biophysica Acta (BBA) - Biomembranes, 1828 (2013) 1153-1158.
[34] Alternative stabilities of a proline-rich antibacterial peptide in vitro and in vivo,

Protein Science A Publication of the Protein Society, 17 (2009) 1249-1255.
[35] Q. Zhang, Y. Xu, Q. Wang, B. Hang, Y. Sun, X. Wei, J. Hu, Potential of novel antimicrobial peptide P3 from bovine erythrocytes and its analogs to disrupt bacterial membranes in vitro and display activity against drug-resistant bacteria in a mouse model, Antimicrob. Agents Chemother., 59 (2015) 2835-2841.
[36] I.M. Gould, A.M. Bal, New antibiotic agents in the pipeline and how they can help overcome microbial resistance, Virulence, 4 (2013) 185-191.
[37] Y. Ma, X. Li, D.M. Li, F.Q. Yan, W. Che, H.P. Sun, Pathogen Distribution and Drug Resistance of Lower Respiratory Tract Infection in Children, Chinese Journal of Nosocomiology, (2010).
[38] W. Zhou, A. Huang, Y. Zhang, Q. Lin, W. Guo, Z. You, Z. Yi, M. Liu, Y. Chen, Design and optimization of hybrid of 2,4-diaminopyrimidine and arylthiazole scaffold as anticancer cell proliferation and migration agents, Eur. J. Med. Chem., 96 (2015) 269-280.
[39] S. National Committee for Clinical Laboratory, Methods for dilution antimicrobial susceptibility tests for bacteria that grow aerobically ; Approved standard, (2003).
[40] W.C. Zeng, Q. He, Q. Sun, K. Zhong, H. Gao, Antibacterial activity of water-soluble extract from pine needles of Cedrus deodara, Int. J. Food Microbiol., 153 (2012) 78-84.
[41] K.P. Devi, S.A. Nisha, R. Sakthivel, S.K. Pandian, Eugenol (an essential oil of clove) acts as an antibacterial agent against Salmonella typhi by disrupting the cellular membrane, J. Ethnopharmacol., 130 (2010) 107-115.
[42] W. Ma, D. Zhang, G. Li, J. Liu, G. He, P. Zhang, L. Yang, H. Zhu, N. Xu, S. Liang, Antibacterial mechanism of daptomycin antibiotic against Staphylococcus aureus based on a quantitative bacterial proteome analysis, J. Proteomics, 150 (2017) 242-251.
[43] K. Xu, S. He, S. Chen, G. Qiu, J. Shi, X. Liu, X. Wu, J. Zhang, W. Tang, Free radical rearrangement synthesis and microbiological evaluation of novel 2-sulfoether-4-quinolone scaffolds as potential antibacterial agents, Eur. J. Med. Chem., 154 (2018) 144-154.
[44] A. Kaushal, K. Gupta, R. Shah, M.L. van Hoek, Antimicrobial activity of mosquito cecropin peptides against Francisella, Developmental & Comparative Immunology, 63 (2016) 171-180.
[45] Y. Li, D.A. Powell, S.A. Shaffer, D.A. Rasko, M.R. Pelletier, J.D. Leszyk, A.J. Scott, A. Masoudi, D.R. Goodlett, X. Wang, LPS remodeling is an evolved survival strategy for bacteria, Proc. Natl. Acad. Sci. USA., 109 (2012) 8716-8721.
[46] D. Teng, X. Wang, D. Xi, R. Mao, Y. Zhang, Q. Guan, J. Zhang, J. Wang, A dual mechanism involved in membrane and nucleic acid disruption of AvBD103b, a new avian defensin from the king penguin, against Salmonella enteritidis CVCC3377, Appl. Microbiol. Biotechnol., 98 (2014) 8313-8325.
[47] A. Kaushal, K. Gupta, M.L.V. Hoek, Characterization of Cimex lectularius (bedbug) defensin peptide and its antimicrobial activity against human skin microflora, Biochemical & Biophysical Research Communications, 470 (2016) 955-960.

[48] W.C. Chu, P.Y. Bai, Z.Q. Yang, D.Y. Cui, S. Qin, Synthesis and antibacterial evaluation of novel cationic chalcone derivatives possessing broad spectrum antibacterial activity, Eur. J. Med. Chem., 143 (2017) 905-921.
[49] B. Liu, H. Huang, Z. Yang, B. Liu, S. Gou, C. Zhong, X. Han, Y. Zhang, J. Ni, R. Wang, Design of novel antimicrobial peptide dimer analogues with enhanced antimicrobial activity in vitro and in vivo by intermolecular triazole bridge strategy, Peptides, 88 (2017) 115-125.

A novel series of phenylthiazole and phenylthiophene pyrimidindiamine derivatives were designed and synthesized.

The structure-activity relationship of target compounds was discussed antibacterial activity against *E. coli* and *S. aureus*.

Compound **14g** has excellent antibacterial activity both *in vitro* and *in vivo*.

Mechanism studies revealed that compound **14g** exerts antibacterial activity by disrupting bacterial cell membranes.

**Conflicts of Interest:** The authors have declared no conflict of interest.